Microbiological Research 218 (2019) 108–117

Contents lists available at ScienceDirect

Microbiological Research

journal homepage: www.elsevier.com/locate/micres

Transcriptome analysis of hopanoid deficient mutant of *Rhodopseuodomonas palustris* TIE-1

Tushar D. Lodha[a,c], Indu B.[a], Sasikala Ch.[b], Ramana Ch.V.[a,*]

[a] Department of Plant Sciences, School of Life Sciences, University of Hyderabad, P.O. Central University, Hyderabad, 500 046, India
[b] Bacterial Discovery Laboratory, Centre for Environment, IST, JNT University Hyderabad, Kukatpally, Hyderabad, 500 085, India
[c] National Centre for Microbial Resource, National Centre for Cell Science, Pune, 411011, India

ARTICLE INFO

Keywords:
Cell membrane
Hopanoids
Rhodopseuodomonas palustris TIE-1
Transport
CRAC motifs
Signal transduction

ABSTRACT

All three domains of life have an ordered plasma membrane which is pivotal in the selective fitness of primitive life. Like cholesterol in eukaryotes, hopanoids are important in bacteria to modulate membrane order. Hopanoids are pentacyclic triterpenoid lipids biosynthesised in many eubacteria, few ferns and lichens. Hopanoid modulates outer membrane order and hopanoid deficiency results in the weakened structural integrity of the membrane which may in turn affect the other structures within or spanning the cell envelope and contributing to various membrane functions. Hence, to decipher the role of hopanoid, genome-wide transcriptome of wild-type and Δ*shc* mutant of *Rhodopseudomonas palustris* TIE-1 was studied which indicated 299 genes were upregulated and 306 genes were downregulated in hopanoid deficient mutant, representing ~11.5% of the genome. Thirty-eight genes involved in chemotaxis, response to stimuli and signal transduction were differentially regulated and impaired motility in hopanoid deficient mutant showed that hopanoid plays a crucial role in chemotaxis. The docking study demonstrated that diguanylate cyclase which catalyses the synthesis of secondary messenger exhibited the capability to interact with hopanoids and might be confederating in chemotaxis and signal transduction. Seventy-four genes involved in membrane transport were differentially expressed and cell assays also explicit that the multidrug transport is compromised in *Δshc* mutant. Membrane transport is reliant on hopanoids which may explain the basis for previous observations linking hopanoids to antibiotic resistance. Disturbing the membrane order by targeting lipid synthesis can be a possible novel approach in developing new antimicrobials and hopanoid biosynthesis could be a potential target.

1. Introduction

Membrane lipids are hydrophobic biomolecules which play a vital role in bacterial cell physiology. Initially, it was thought that membrane lipids are the static barrier. But with advanced findings, it is recognized as a complex and dynamic component of the membrane which selectively connects cell with its extracellular environment. In eukaryotes, lipid raft organizes signal transduction proteins which are enriched in specific lipids such as cholesterols (López and Kolter, 2010). Lipid rafts can sense extracellular signals, and they support different cellular processes, including cell cycle, cytoskeleton rearrangement, signal transduction, vesicle trafficking and cellular homeostasis (Barak and Muchova, 2013; Bramkamp and Lopez, 2015). Sterol lipids (cholesterol and its derivatives) are widely distributed in a eukaryotic system and form a vital component of membrane lipids along with phospholipids and sphingolipids which play a key role in signal transduction and various membrane functions (Hannich et al., 2011). Prokaryotes contain lipid rafts (microdomains) but sterols are absent in prokaryotic members with few exceptions (Wei et al., 2016). But bacteria harbour hopanoid which is widespread of all complex natural products and analogous to sterols and are probably an essential constituent of many prokaryotes (Blumenberg et al., 2012, 2010; Doughty et al., 2009; López and Kolter, 2010; Rohmer et al., 1984; Saenz et al., 2012b; Wei et al., 2016).

Abbreviations: ATP, Adenosine triphosphate; BCAA, Branched chain amino acid; CARC, CRAC like motif; CCCP, Carbonyl cyanide m-chlorophenyl; CRAC, Cholesterol recognition amino acid consensus; DMSO, Dimethyl sulfoxide; GO, Gene Ontology; H33342, Bisbenzimide H33342; MPP1, Membrane palmitoylated protein; NPN, N-phenyl-naphthylamine; OD, Optical density; PBS, Phosphate buffer saline; PDB, Protein Data Bank; PDZ, Post-synaptic density; qPCR, Quantitative polymerase chain reaction; *shc*, squalene hopene cyclase; TBDT, TonB-dependent transport system; WT, Wild-type; YP, yeast extract, peptone; YPP, Yeast extract, peptone and pyruvate

* Corresponding author: Department of Plant Sciences, School of Life Sciences, University of Hyderabad, P.O. Central University, Hyderabad, 500 046, India.
E-mail addresses: cvr449@gmail.com, cvramana449@gmail.com (R. Ch.V.).

https://doi.org/10.1016/j.micres.2018.10.009
Received 4 July 2018; Received in revised form 20 September 2018; Accepted 27 October 2018
Available online 29 October 2018
0944-5013/

Hopanoids are pentacyclic isoprenoid lipid molecule biosynthesised in many eubacteria as well as few higher plants, protists, ferns, mosses, and fungi (Blumenberg et al., 2009; Cvejic et al., 2000; Kannenberg et al., 1995; Rohmer et al., 1984; Silipo et al., 2014; Talbot et al., 2008; Tank and Bryant, 2015). Though not extensively studied, hopanoids contribute to the membrane stability, membrane permeability, progressions in cell cycle, plant-microbe interactions, resistance to antibiotics and help in stress tolerance (Doughty et al., 2011; Kulkarni et al., 2013, 2015, Saenz et al., 2015, 2012a, 2011; Welander et al., 2009). However, the role of hopanoid is not conclusively elucidated and the extent to which they are sterol surrogate remains an open question. A robust interpretation of cellular functions of hopanoids is required to better understand their physiological significance. Therefore, to gain insights into the role of hopanoids in bacteria, the global transcriptional study of hopanoid deficient mutant of *R. palustris* TIE-1 was carried out and few of the traits were experimentally validated. Here, we report that the hopanoid deficiency leads to an alteration in the membrane transport, especially energy-dependent multidrug transport system. This study describes for the first-time, the possibility of interaction between hopanoids and diguanylate cyclase which might be involved in various cellular processes in *R. palustris* TIE-1. Hopanoids thus confederate in membrane transport, chemotaxis and signal transduction in *Rhodopseudomonas palustris* TIE-1.

2. Materials and methods

2.1. Organisms and growth condition

Wild-type and *Δshc* mutant of *R. palustris* TIE-1 (Welander et al., 2009) were grown at 30 °C in light with 2,400 lx in YP medium (0.3% yeast extract and 0.3% peptone) maintaining micro-aerobic conditions in the screw cap test tube. The growth analysis of *Δshc* mutant and wild-type (WT) strain of *R. palustris* TIE-1 was carried out in YP media with different carbon sources (succinate, pyruvate, acetate and malate at 10 mM concentration). Exponential growth phase cells normalised to 0.5 at OD_{660nm} were inoculated (1% inoculum) in triplicate into the appropriate medium. The growth was monitored over time by measuring absorbance at 660 nm. The growth of *Δshc* mutant was least affected in pyruvate (YPP media) containing media; therefore further study was carried out in YPP media.

2.2. RNA isolation and microarray experiment

WT and *Δshc* mutant of *R. palustris* TIE-1 were grown in YPP media. The cells were harvested from the mid-log growth phase for the microarray experiment. By harvesting cells in mid-log phase, the inconsistency between the strains due to altered growth rates and morphologies were minimized (Welander et al., 2009). The experiment was carried out in triplicate, each with three biological replicates. Three biological replicates from the individual experiment were pooled together to minimize biological variation. Cells (10 ml each) were harvested by centrifugation (4 °C, 10000 g for 3 min) and washed twice with PBS buffer. The cell pellet was snap frozen immediately in liquid nitrogen and stored at −80 °C until further process. RNA was isolated using Qiagen RNeasy Mini kit, and RNA quality (integrity and DNA contamination) was checked by Agilent 2100 Bioanalyzer. Isolated RNA was treated with DNase using on-column DNase treatment as per manufacturer's instructions. The RNA was eluted with 20 µl of nuclease-free water and stored at −80 °C until further use.

The microarray chip with the 8 × 15k array with 5245 different probes were designed and etched by Affymetrix. Oligo dT primer was used to reverse transcribe total RNA and dye Cy3 was incorporated while cRNA preparation was carried out by the in vitro transcription. The labeled cRNA was cleaned up using Qiagen RNeasy Mini kit columns as per manufacturer's instructions (Qiagen, USA). Gene expression hybridisation kit (Agilent Technologies) was used for fragmentation and hybridisation. In brief, 500 ng of labeled cRNA samples were fragmented at 60 °C and hybridized on to Agilent *Rhodopseudomonas palustris*_GXP_8 × 15k (AMADID: 75878) array format. Hybridization was carried out at 65 °C for 16 h and wash buffer (Agilent Technologies) was used to wash hybridised slides.

2.3. Microarray data analysis

Data extraction from images and quantification were carried out using Feature Extraction software version 11.5 (Agilent Technologies). Feature extracted raw data was analysed using GeneSpring GX software version 13.0 (Agilent Technologies). Fold change was calculated as logarithmic values with $\log_2$. Pathway analysis of the differentially regulated genes was performed using DAVID database (Dennis et al., 2003).

2.4. Network construction, visualization, and analysis

PheNetic algorithm was used to construct the subnetwork from the differentially expressed genes as a perturbation of hopanoid deficiency in *R. palustris* TIE-1 (De Maeyer et al., 2013). Cytoscape 3.0 was used for the analysis and visualization of the network. Gene Ontology (GO) annotation for *R. palustris* TIE-1 was downloaded from UniProt website (www.uniprot.org).

2.5. Swimming motility assay

To understand whether weak cell membrane in hopanoid deficient mutant affects the cell motility, swimming motility assays were performed according to Schmerk et al. (2011). For swimming assays, 2 µl of overnight grown culture, adjusted to OD_{660nm} of 0.5, was inoculated in the agar swim plate (YPP with 0.3% agar). The plates were incubated at 30 °C for 96 h, after which the diameter of the swimming motility was measured.

2.6. NPN uptake assay

To test whether hopanoid deficiency leads to defective membrane permeability and transport, N-phenyl-naphthylamine (NPN; Sigma, 104043) uptake assay was carried out (Saenz et al., 2015). *R. palustris* TIE-1 (WT and *Δshc* mutant) cultures were grown for 96 h and harvested by centrifugation (5,000 g for 10 min) under sterile conditions. The pellet was washed with mineral media, and final OD_{660nm} was adjusted to 0.5. 180 µl of cells were transferred to the 96-wells microtiter plate. Before NPN (5 µM) was added the background signals were measured for 15 min. Fluorescent emission readings were recorded after every 5 min, with 25 s shaking till 300 min. The emission of NPN was recorded at excitation = 340/25 nm and emission = 450/8 nm. The entire assay was performed at room temperature. Pyruvate was added at 10 mM concentration whereas control was without a carbon source.

2.7. H33342 ATP-dependent efflux assay

To understand the energy-dependent transport in *Δshc* mutant, ATP-dependent efflux assay was carried out (Saenz et al., 2015). WT and *Δshc* mutant were grown for 96 h at 30 °C. Cells were harvested by centrifugation (5,000 g for 10 min) and washed once with mineral media. All the following wash steps and resuspensions were performed in mineral media containing 5 µM H33342 (Bisbenzimide H 33342; ThermoFisher Scientific, H1399). The OD_{660nm} was normalized to 0.5 and carbonyl cyanide m-chlorophenyl (CCCP; 100 µM; Sigma, C2759) was added to abolish ATP synthesis. The 1% DMSO (HiMedia, MB058) did not inhibit the growth of strain TIE-1 or *Δshc* mutant. The mixtures were incubated in darkness for 1 h, washed twice to remove CCCP, and then resuspended in mineral media and normalized to OD_{660nm} of 0.5.

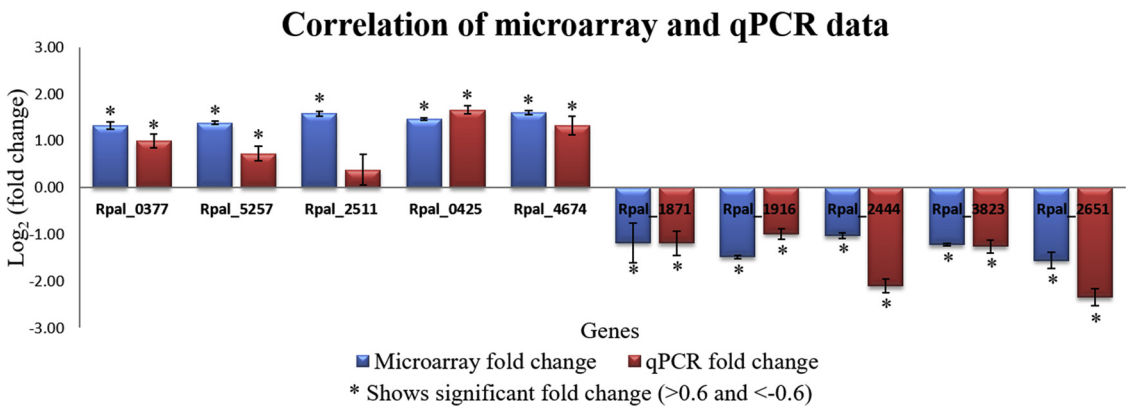

Fig. 1. Correlation of microarray and qPCR data for few genes of *R. palustris* TIE-1. Blue colour indicates the fold change calculated from microarray data and red colour indicates the fold change from qPCR experiments. Microarray experiment was done in duplicate and qPCR experiment was done in triplicate. Rpal_0377-thioredoxin; Rpal_5257-33 kDa chaperonin; Rpal_2511-putative monooxygenase protein; Rpal_0425-cytochrome P450; Rpal_4674-osmC family protein; Rpal_1871-methyl-accepting chemotaxis sensory transducer with PAS/PAC sensor; Rpal_1916-diguanylate cyclase; Rpal_2444-diguanylate cyclase/ phosphodiesterase with PAS/PAC sensor; Rpal_3823-Sodium/hydrogen exchanger; Rpal_2651-TonB dependent receptor.

Bacterial suspension (180 µl) was transferred to the 96-well microtiter plate. The initial concentration of H33342 was noted for 60 min in a plate reader (excitation = 340/25 nm, emission = 405/8 nm). Afterward, pyruvate was added to a final concentration of 20 mM (5 µl of 740 mM solution) per well, and the change in H33342 emission was recorded after every 5 min, with 25 s of shaking for an additional 240 min.

2.8. Protein modeling and docking experiments

Protein sequence for Rpal_1916 and Rpal_2444 was retrieved from the NCBI database. TMHMM2 (http://www.cbs.dtu.dk/services/TMHMM/) were used for the prediction of transmembrane helices and EMBOSS:fuzzpro was used to search cholesterol recognition amino acid consensus (CRAC) and CRAC-like (CARC) motif in proteins. The hydrophobicity plot was plotted using ProtScale server (http://web.expasy.org/protscale/). The PDB (protein data bank) structure of the MPP1 protein was shared by Prof. Aleksander F. Sikorski, the PDB structure of diguanylate cyclase (4RNH) was downloaded from PDB database (www.rcsb.org) and the homology model for Rpal-2444 and Rpal_1916 was generated using SWISS model and I-TASSER, respectively. The docking of cholesterol, diplopterol, diploptene and tetrahymanol was carried out using PyRx software and docking was visualized using discovery studio software and PyMol software.

3. Results

3.1. Growth study of WT and Δshc mutant

Δ*shc* mutant of *R. palustris* TIE-1 did not produce any hopanoids and whereas complement strain produces all the hopanoids (Welander et al., 2009). In *R. palustris* TIE-1, hopanoids are not necessary for growth but hopanoid deficiency leads to severe growth defect and membrane damage in stress conditions (Welander et al., 2009). To study the physiological response of hopanoid deficiency in *R. palustris* TIE-1, growth assays were performed for WT and Δ*shc* mutant grown in the microaerophilic condition in different carbon sources. In comparison to WT, Δ*shc* mutant showed differential behaviour when grown in a medium supplemented with different carbon sources (succinate, pyruvate, malate and acetate; Supplementary Fig. S1 online). In all the tested carbon sources, the growth of Δ*shc* mutant was slow as compared to wild-type strain. Since the behaviour of WT and Δ*shc* mutant strains were almost identical in the presence of pyruvate containing media, YPP media was used for culturing WT and Δ*shc* mutant in further study. To understand physiological changes of *R. palustris* TIE-1 in the absence of hopanoid biosynthesis, the genome-wide transcriptome of WT and Δ*shc* mutant was studied.

3.2. Transcriptional response of Δshc mutant of R. palustris TIE-1

3.2.1. Overview of microarray data analysis

The microarray experiment was carried out for WT and Δ*shc* mutant grown in YPP media. For microarray experiment, WT and Δ*shc* mutant cells were harvested from the mid-log phase which minimizes the inconsistency between the strains due to altered growth rates and morphologies. The scatter plot and principal component analysis was carried out to understand the quality of replicates and experimental data. Microarray experiment showed that in hopanoid deficient mutant of *R. palustris* TIE-1, 299 genes were upregulated and 306 genes were downregulated with respect to WT (Supplementary Table S1 and S2 online) which represents 11.5% of genes in the genome. Various uncharacterised protein-coding genes were differentially expressed (Supplementary Table S3 and S4 online). To check the quality of microarray experiment, 10 genes were selected, and qPCR was carried out. Out of 10 genes, fold change for 9 genes was in accordance with the with microarray data, whereas *Rpal_2511* gene did not show significant differential expression (Fig. 1).

3.2.2. Functional annotation of differentially expressed genes

To comprehend insights into the transcriptional response of *R. palustris* TIE-1 during hopanoid deficiency, the Gene Ontology (GO) classification was used to enrich genes related to the specific functional group. The function and pathway analysis were done for differentially regulated genes using DAVID database (Dennis et al., 2003). It was observed that genes belonging to processes such as oxidation-reduction, cell redox homeostasis, proteolysis, electron carrier activity, ABC transporters, glyoxylate and dicarboxylate metabolism, fatty acid metabolism, and monooxygenase were upregulated (Supplementary Table S1 online). It was also found that genes belonging to processes such as regulation of transcription, membrane transport activity, ABC transporters, plasma membrane, two-component system, bacterial chemotaxis, nitrogen metabolism and amino acid metabolism were downregulated (Supplementary Table S2 online).

3.2.3. Subnetwork analysis

To understand how the hopanoid deficiency could affect cellular response, a subnetwork selection algorithm, PheNetic, was used to construct subnetwork based on differentially expressed genes. A possible interaction network representing interactome of nearest strain *R. palustris* CAG009 was compiled from string actions networks and

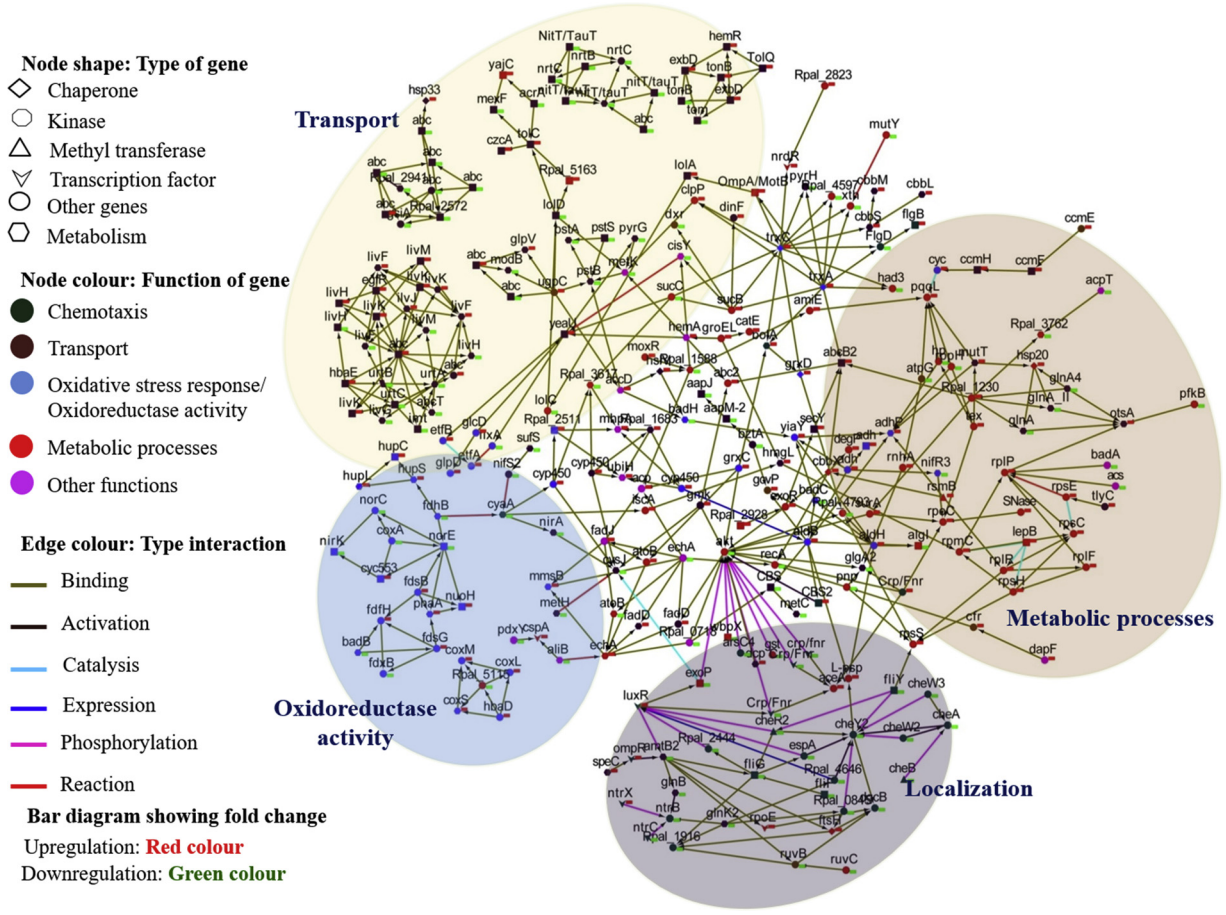

Fig. 2. Hopanoid deficiency triggers transcriptional changes. Shown is selected subnetwork based on the differentially expressed genes in the Δ*shc* mutant of *R. palustris* TIE-1. The PheNetic algorithm was used to select subnetwork from 605 differentially expressed genes. Subnetwork consists of 262 nodes and 438 nodes, 219 differentially expressed genes and additional 43 intermediate genes which were selected by PheNetic. The shape of the node represents the type of gene, colour of node represents the function of gene, colour of edge represents the type of interaction and bar diagram besides the nodes corresponds to fold change.

mapped on *R. palustris* TIE-1 genome. Using this network, a minimal common subnetwork was constructed by the PheNetic algorithm which connects a cause (hopanoid deficiency) to differentially expressed genes (its effect). From the differentially expressed genes subnetwork was constructed which consisted of 266 nodes (genes) and 408 edges (interactions). From the subnetwork, it was observed that the gene network involved in membrane transport, localization and oxidoreductase activity was greatly affected in hopanoid deficient condition in *R. palustris* TIE-1 (Fig. 2).

3.2.4. Cellular response of Δshc mutant

3.2.4.1. Membrane transport. In Δ*shc* mutant of *R. palustris* TIE-1, 74 genes involved in transport activity were differentially expressed which suggest that hopanoids might be playing a role directly or indirectly in membrane transport (Fig. 2; Supplementary Table S2 online). In *Streptomyces cremoris*, it was established that the membrane lipid composition affects the transport protein of branched-chain amino acids (BCAAs) like leucine, isoleucine and valine (Driessen et al., 1987). Twenty-three genes participating in BCAAs were differentially expressed in Δ*shc* mutant. BCAA transport system is a part of osmotic shock-sensitive transporters which rely on periplasmic binding proteins (Quay and Oxender, 1979). Genes involved in TonB dependent transport system (TBDT) was downregulated in Δ*shc* mutant. TBDTs catalyses the active transport of iron-siderophore complexes, vitamin B_{12}, nickel complexes, carbohydrates, group B colicins and bacteriophages T1 and ø80 through high-affinity transporters in the outer membrane (Noinaj et al., 2010). The *fur* gene that encodes a regulatory protein got upregulated in the Δ*shc* mutant, which represses genes required for iron uptake which is reported in oxidative stress. Iron uptake is reported to alter with the change in proton motif force and oxidative stress (Noinaj et al., 2010). Therefore, altered TBDT may be the result of defective proton motive force and oxidative stress in an impaired membrane of Δ*shc* mutant of *R. palustris* TIE-1. Similarly, seven genes involved in nitrate transport were downregulated which depends on ATP hydrolysis and proton-motive force (Noinaj et al., 2010).

Similarly, 11 genes subnetwork involved in dipeptide and oligopeptide transport was downregulated in Δ*shc* mutant. Four genes encoding for extracellular solute-binding proteins which are involved in the transport system, sensing chemicals (chemoreceptors) and initiators of the signal transduction pathway (Tam and Saier, 1993) were downregulated. This gene network triggered the high expression of 33 kDa chaperonin which is a redox-regulated molecular chaperone. 33 kDa chaperonin plays a crucial role in the protection of oxidatively damaged proteins and bacterial defence system in oxidative stress (Jakob et al., 1999). Polyamine transport system was also downregulated in the Δ*shc* mutant. Polyamines are polycationic molecules which interact with negatively charged nucleic acid and are linked to protection of a cell from oxidative and acid stress (Shah and Swiatlo, 2008). ATP-dependent zinc metallopeptidase (*Rpal_1317*) was upregulated which is involved in quality control of integral membrane proteins. The transport of polar amino acid was also downregulated in Δ*shc* mutant.

Twenty-three ABC transporters were downregulated in Δ*shc* mutant,

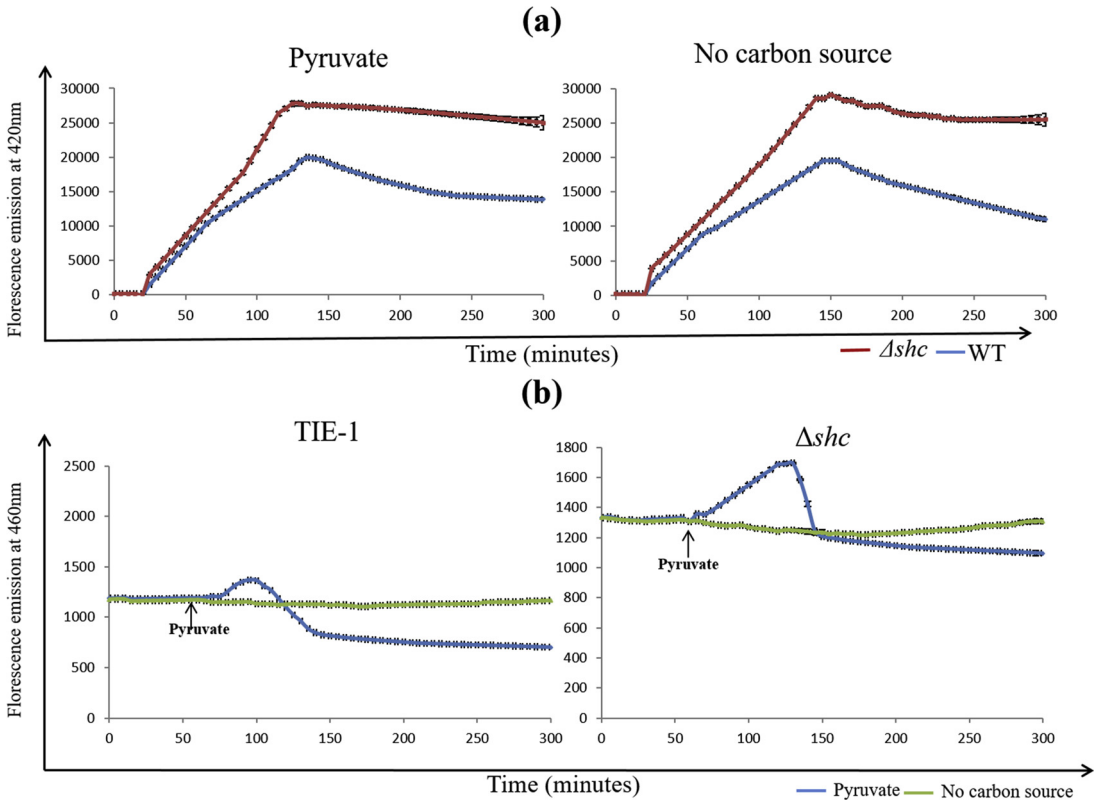

Fig. 3. (a) The membrane permeability was assessed by NPN uptake assay which is monitored by the accumulation of the NPN (lipophilic dye) in the cell. (b) Energy-dependent multidrug transport was assessed by ATP-dependent efflux assay which is monitored by efflux of fluorescent dye (H33342). Each reading represents the average of three replicates (the error bars represents standard deviation). NPN uptake assay was repeated three times.

therefore to test whether hopanoid deficiency leads to defected membrane permeability and transport, NPN uptake assay was carried out. The nonpolar NPN is a fluorescent probe which has a property of phospholipid environment sensitive spectral shifts enabling studies of the permeability of the outer membrane of Gram-stain-negative bacteria (Loh et al., 1984). In NPN uptake assay, it was observed that in WT strain (pyruvate containing) fluorescence signal increases up to 130 min after which it started decreasing with time (Fig. 3a). Equivalent results were obtained in cells incubated without a carbon source. NPN fluorescence is high in the phospholipid environment and initial increase in fluorescence and then decrease in fluorescence is an indication of the active efflux of dye from the cell which is characteristically observed in bacteria. In contrast, in damaged outer membrane of the cell, NPN gets accumulated more (compared to healthy cells) with time and results in prominent fluorescence and the fluorescence doesn't change with time. In *Δshc* mutant, in both pyruvate and without carbon sources it was noted that the fluorescence signal increased exponentially till 120 min and became constant with time (Fig. 3a). This indicated that the dye entered the cells of *Δshc* mutant and incorporated in the cell membrane and accrue without effluxing the dye out of cell which shows that membrane transport is impaired in hopanoid deficient cells.

ATP-dependent efflux assay was performed for WT and *Δshc* mutant of *R. palustris* TIE-1. The cells were stained with nucleic acid dye H33342 followed by inhibiting ATP synthesis using CCCP; cells were washed to remove excess dye and inhibitor. Fluorescence readings were taken for 60 min which indicated no variation in the fluorescence demonstrating inhibition of ATP biosynthesis by CCCP. Pyruvate was added to restore the ATP biosynthesis. In healthy cells stained with H33342, ATP biosynthesis will be restored as soon as a carbon source is added and thus the cell will start effluxing the dye out resulting in a decrease in fluorescence. Fluorescence started increasing in WT strain after adding pyruvate and with time fluorescence signal decreased, indicating restoration of ATP synthesis efflux of fluorescent dye H33342 out of the cell. In the *Δshc* mutant the initial fluorescence was high compared to WT and after adding pyruvate, fluorescence started increasing and subsequently started decreasing but did not reduce significantly and remains above control (Fig. 3b). In control (without pyruvate), the fluorescence remains constant throughout the experiment indicating ATP synthesis was abolished.

3.2.4.2. Oxidation reduction and electron carrier activity. Oxidation and reduction reactions play a crucial role in cellular respiration. Nineteen genes which are involved in the oxidation-reduction process were found to be upregulated in *Δshc* mutant (Supplementary Table S2 online). Various enzymes act as electron acceptors as well as donors and take part in electron transport chain generating an electrochemical gradient across the cell membrane. In *Δshc* mutant, 21 genes which are involved in electron carrier activity were also upregulated (Supplementary Table S1 online). Six genes involved in monooxygenase activity and also takes part in electron carrier activity were also upregulated in *Δshc* mutant. Twenty-eight genes involved in cellular homeostasis and oxidoreductase activity were upregulated. Bacterial thioredoxins are small redox proteins which are linked cellular redox regulation and oxidative stress defence mechanisms.

3.2.4.3. Chemotaxis, response to stimulus and flagellar assembly. Microarray data showed that 38 genes involved in response to external stimuli, chemotaxis and flagellar assembly were downregulated in *Δshc* mutant (Supplementary Table S2 online). Seven genes involved in flagellar assembly and motility showed significant downregulation in hopanoid deficient mutant. Hence, swimming assay was carried out to understand the defect in motility. In swimming motility assay, the diameter of motility was same for WT and *Δshc* mutant within the first 48 h but after 96 h swimming motility

was reduced in *Δshc* mutant (Supplementary Fig. S2 online).

3.2.4.4. Interaction between proteins and hopanoids. Cholesterol interacts with the PDZ domain-containing proteins and modulates cell signaling and protein network. PDZ domain-containing scaffold proteins have been stated to interact with cholesterol which contains CRAC and CARC motifs (Listowski et al., 2015; Sheng et al., 2012). Hopanoids play a crucial role in maintaining integrity (regulating the physical properties) of a cell membrane and might be physically interacting with few proteins controlling their action similarly as the cholesterol does in eukaryotes. Membrane palmitoylated protein 1 (MPP1) of *Homo sapiens* is known to interact with cholesterol and play a pivotal role in lateral membrane organisation in lipid rafts (Listowski et al., 2015). Cholesterol is structurally analogous to hopanoids; therefore, to test the hypothesis that whether MPP1 can interact with hopanoids *in-silico* docking experiment was carried out. MPP1 protein has 17 CRAC motifs and 14 CARC motifs (CRAC-like motif) which were predicted using EMBOSS: fuzzpro server (Supplementary Table S5 online). *In-silico* docking experiments suggested that diplopterol, diploptene and tetrahymanol can dock to the MPP1 protein similar to what cholesterol does (Supplementary Fig. S3 online). This indicates that hopanoids mimic cholesterol molecule and have the capability to interact with a protein having CRAC motif.

With the MPP1 protein, it was contemplated that the hopanoid mimics the cholesterol in terms of binding to CRAC motif in proteins. Therefore, it was interesting to understand whether bacterial proteins have CRAC or CARC motif which can interact with hopanoids in similar faction as cholesterol do and contribute to the signal transduction. Genome sequence of *R. palustris* TIE-1 was mined for the CRAC/CARC motif-containing proteins, and it was observed that *R. palustris* TIE-1 have many proteins with CRAC motifs (Supplementary Table S6 online). The genome of *R. palustris* TIE-1 consists of 34 genes which code for diguanylate cyclase having PDZ domain out of which two got significantly downregulated in hopanoid deficient mutant of *R. palustris* TIE-1. Diguanylate cyclase (Rpal_1916 and Rpal_2444) has PDZ domain-containing CRAC motifs which are known to be involved in interaction with cholesterol and controls cell signaling and protein networking (Sheng et al., 2012). So, there might be a possible interaction between diguanylate cyclase having CRAC motif and hopanoids. Diguanylate cyclases which were differentially expressed in *Δshc* mutant were further selected for docking study.

Rpal_2444 protein has 17 CRAC and 18 CARC motifs (Table 1). NCBI-BLAST of Rpal_2444 protein sequence against the PDB database showed 40% identity with diguanylate cyclase (PA4601) of *Pseudomonas aeruginosa* PAO1 (PDB_ID: 4RNH) which has 12 CRAC motifs and 13 CARC motifs (Table 1). Diguanylate cyclase from *Pseudomonas aeruginosa* PAO1 has 1415 amino acids with four PAS sensory domain, phosphodiesterase and diguanylate cyclase (DGC) domain (Phippen et al., 2014). Crystal structure of PA4601 was elucidated for the fragment spanning from 978 to 1409 amino acids which are 431 amino acid long fragment comprise of DGC activity (Phippen et al., 2014). Three-dimensional structure was used to study the *in-silico* binding affinity for ligands (cholesterol, diplopterol, diploptene and tetrahymanol). Nine CRAC motifs are spanned throughout the protein sequence of PA4601 (Fig. 4). Out of 9 CRAC motifs comprising domain, five domains did not show binding for any of the ligands tested. Other four CRAC motifs with sequence 190-LHYQPQFTGDGRR-202, 270-RQFADGQL-277, 337-LNYLKQFPIDVLKIDRSFVDGL-358 and 404-VQGYLFGR-412 are part of one pocket in the three-dimensional structure of a protein (Fig. 4 and Supplementary Table S5 online). Cholesterol, diploptene, diplopterol and tetrahymanol has shown binding in the above pocket with binding energy -7.2 kcal/mol, -8.7 kcal/mol, -8.3 kcal/mol and -8.3 kcal/mol, respectively (Fig. 4c). The interacting amino acids are different for all ligands and ligand confirmation also differ for each ligand (Supplementary Table S7 online).

Therefore, it was paramount to test whether diguanylate cyclase (Rpal_2444) from *R. palustris* TIE-1 also has the capability to interact with hopanoids. The homology model of Rpal_2444 was generated using SWISS model server using 4RNH as a template. The deduced amino acid sequence of Rpal_2444 has 673 amino acid residues. The three-dimensional structure of this protein was comprised of 417 (242 to 659) amino acids. The sequence alignment has shown that the GGDEF domain is conserved whereas DDFGTG domain got altered to DDFGAG in Rpal_2444 which was highlighted in Fig. 5. According to the Ramachandran plot, 97.3% residues were in the favoured region, 1% residues were in additionally allowed regions and 1.7% residues were in the outliner regions indicating a good stereochemical quality of the model. *In-silico* docking experiments were performed to test whether cholesterol, diplopterol, diploptene and tetrahymanol bind to these motifs. Similar to PA4601 four CRAC/CARC motifs (from 445 to 452, 498 to 517, 574 to 595 and 641 to 648 amino acids) are lying in the close vicinity and forming a pocket. *In-silico* docking experiment has shown that Rpal_2444 can interact with the hopanoids and cholesterol in the same pocket spanning 445-VGFEALLR-452, 498-LAIAVNFSPLDFRRFDVPAL-517, 574-LSYLQSFPFDKIKIDQAFTRKL-597 and 641-VQGYLIGR-648 (Fig. 5c). Binding energy was maximum for diplopterol which is -8.5 kcal/mol followed by diploptene (-8.1 kcal/mol), tetrahymanol (-7.6 kcal/mol) and tetrahymanol (-6.7 kcal/mol). The orientation of ligands and interacting amino acids are different for

Table 1
Predicted CRAC/CARC motif in Rpal_2444 and Rpal_1916 of protein of *R. palustris* TIE-1 and homologous diguanylate cyclase of *Pseudomonas aeruginosa* PAO1 (PA4601).

Sequence	Start	End	Number of CRAC/CARC motif
Rpal_2444			
LGVVAAYGGLR	25	35	3
LDIYGIPPGR	149	158	1
RGFCLFDAVGRL	130	141	3
KQAEQRFAYLALHDVATGLPNRAAFNDRIV	233	262	6
RRFDGSFAVIRLGIDRFKEINDVFGQAV	269	296	6
RPGGDEFSIV	319	328	1
LCDTEFEVDGHR	348	359	1
VSVYPR	368	373	1
VALYRAK	387	393	1
RGTVCLFEPAMDL	397	409	1
VGFEALLR	445	452	2
LAIAVNFSPLDFRRFDVPAL	498	517	4
LSYLQSFPFDKIKIDQAFTRKL	574	595	5
VQGYLIGR	641	684	1
4RNH			
RGSHMAYYDAL	17	27	1
LPNRTLFQDRL	30	40	2
VVLMFLDLDR	54	63	3
RMGGDEFTLLL	99	109	3
RLARPFTLEGREFFV	132	146	3
LHYQPQFTGDGRR	216	228	2
RQFADGQL	296	303	1
LNYLKQFPIDVLKIDRSFVDGL	363	384	7
LDFLR	419	423	1
VQGYLFGR	430	437	1
Rpal_1916			
RWIGLFGCV	43	51	1
KAAARYLL	127	134	1
VLVAFTAFTGR	140	150	3
KLDYPGYSLHLKRQFIGVL	229	247	9
LTNYLGEIYR	260	269	1
RFDQAFFVV	424	432	2
RRDELFRTL	443	451	2
LQIAEQFGASGR	460	471	1
REIFGGDWVEFGGRRSYVL	476	494	5
VKGIFASRLL	511	518	3
LFYFFGMDRGVRDRFERQLR	533	552	5
LANRMKFDARL	574	584	2
RSGRPFSLIIFDIDHFKEVNDIYGHPV	593	619	4
RWGGEEFAILL	643	653	2
RADNALYRAKL	704	714	1

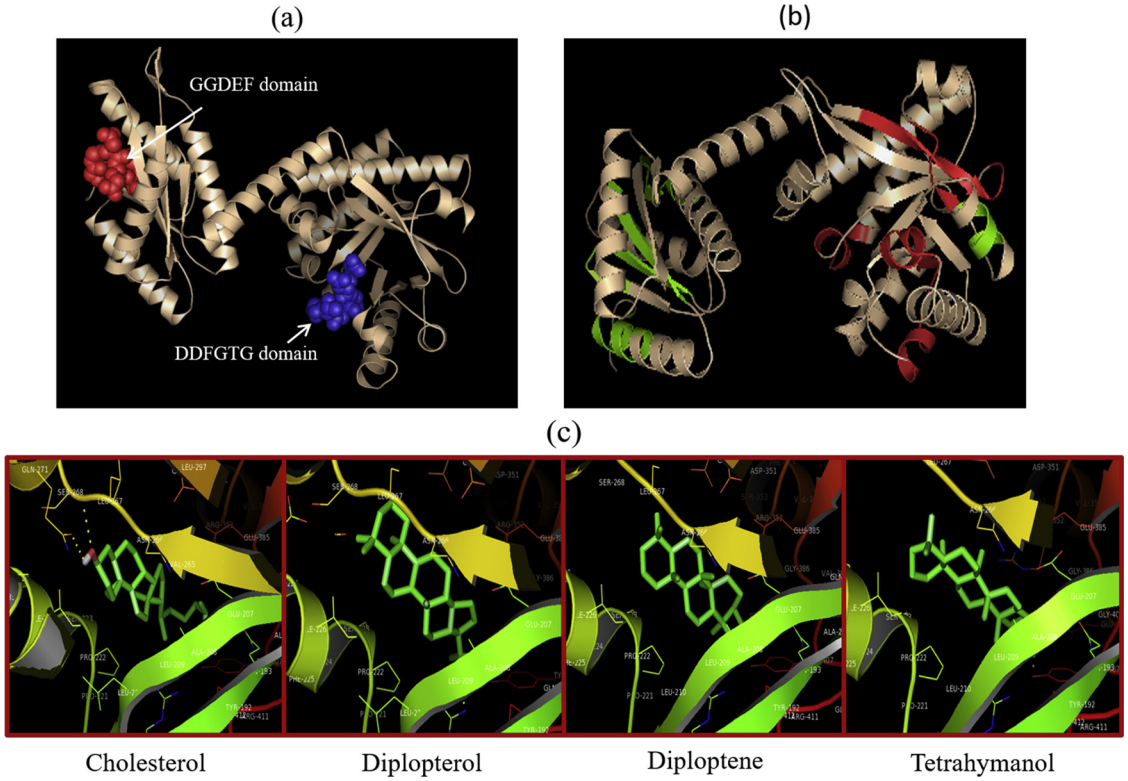

Fig. 4. (a) Three-dimensional structure of PA4601 (978–1409 amino acids) with (a) heighted GGCEF domain (red colour) and DDFGTG domain (blue colour) (b) CRAC/CARC motif (green colour) with CRAC motif showing binding for hopanoids and cholesterol highlighted with red colour and (c) Visualisation of binding of ligands with diguanylate cyclase (PDB ID-4RNH) of *Pseudomonas aeruginosa* PAO1.

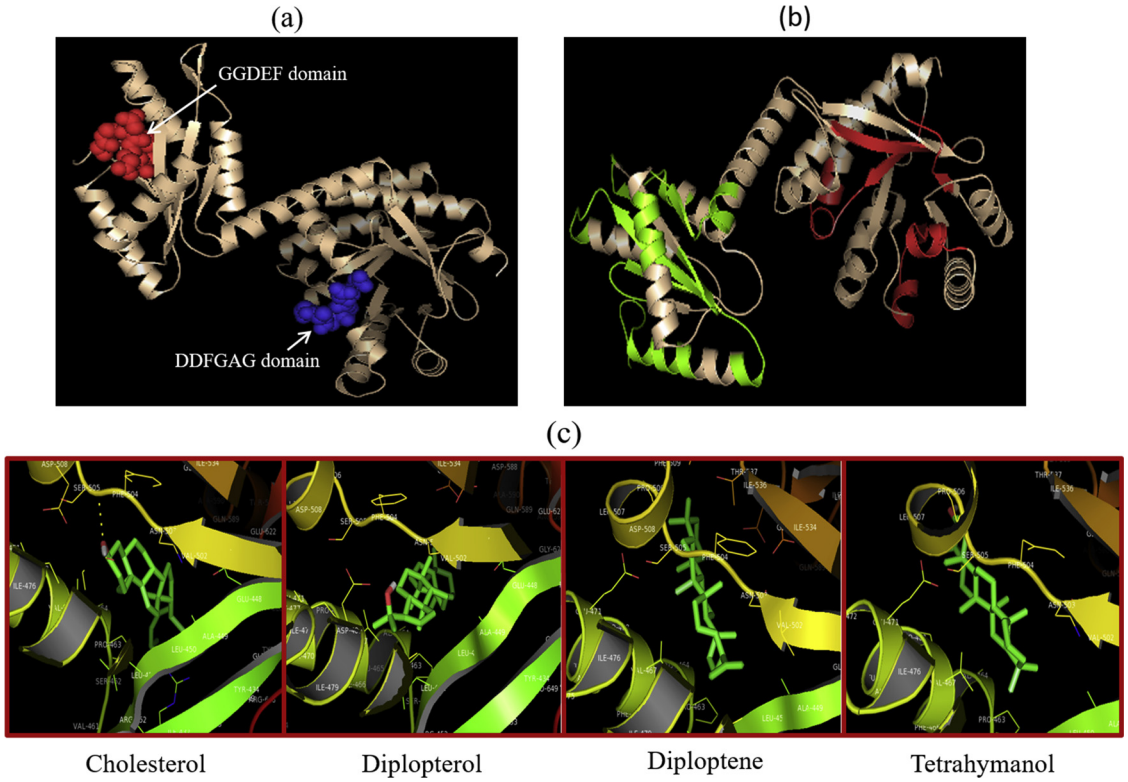

Fig. 5. (a) Three-dimensional structure of Rpal_2444 with (a) heighted GGCEF domain (red colour) and DDFGAG domain (blue colour) (b) CRAC/CARC motif (green colour) with CRAC motif showing binding for hopanoids and cholesterol highlighted with red colour and (c) Visualization of binding of ligands with Rpal_2444 protein of *R. palustris* TIE-1 CARC/CARC motif spanning from 445 to 452, 498 to 517, 574 to 595 and 641 to 648 amino acids.

individual ligands tested (Supplementary Table S7 online).

The deduced amino acid sequence of Rpal_1916 has 736 amino acid residues. The protein has very poor homology with the already elucidated structure of diguanylate cyclase (Pfl01_4666) of *P. fluorescence* Pf0-1 with PDB_ID: 5EUH. Hence, the threading approach was used to model the protein Rpal_1916 using I-TASSER server (Zhang, 2008). The deduced three-dimensional structure was refined using GalaxyRefine tool (Heo et al., 2013) and the resulted structure has 736 amino acid residues. The sequence alignment has shown that the GGDEF domain is replaced with GGEEF in both the sequences. According to the Ramachandran plot, 656 (89.4%) residues were in the favoured region indicating the stereochemical quality of the model. Rpal_1916 protein has 15 CRAC motifs and 26 CARC motifs (Table 1). TMHMM has shown that in Rpal_1916 protein, there are eight possible regions which might be buried in the cell membrane (Supplementary Fig. S4 online).

In-silico docking experiments were performed to test whether cholesterol, diplopterol, diploptene and tetrahymanol binds to CRAC motifs in Rpal_1916. The motif having amino acid sequence 140-VLVAFTAF-TGR-150 showed binding for only cholesterol molecule (binding energy -9.1 kcal/mol) whereas hopanoids tested did not show binding in this region which is predicted as a part of a transmembrane helix. Diplopterol has not shown binding in regions spanning CRAC motifs whereas it has shown binding to Rpal_1916 in a region which is part of transmembrane helix with binding energy -10 kcal/mol. The region with CRAC motif and transmembrane helix increases the probability of interaction between cholesterol (maybe same for hopanoids) and proteins (Listowski et al., 2015). There are few reports stating that cholesterol interacts with the membrane protein in a region other than CRAC motif (Fantini and Barrantes, 2013). All the other ligands had also demonstrated binding confirmation in the same regions (Data not shown). Diploptene and tetrahymanol have demonstrated binding in CRAC motif having sequence 476-REIFGGDWVEFGGRRSYVL-494 which consist of 5 CRAC motifs. Diploptene has shown the binding energy of -8.2 kcal/mol in this region and also involved few residues of other CRAC motif spanning from 460 to 471 and 533 to 522 amino acids (Supplementary Fig S5 online). Tetrahymanol has demonstrated binding energy of -9.3 kcal/mol for the interaction with CRAC motif spanning from 476 to 494 amino acid residues and also encompasses few amino acids of CRAC motif spanning from 229 to 247 amino acids (Supplementary Fig S5 online).

4. Discussion

All domains of life have ordered cell membrane which is essential for the selective fitness of primitive life. Reduced membrane order may alter the membrane-associated functions such as membrane transport, cell signaling and results in susceptibility to bilayer-disrupting agents (Saenz et al., 2015, 2012a). Hopanoids are known to interact with lipid A to promote order in the outer membrane which is similar to the interaction between sterols and sphingolipids in the eukaryotic membrane (Silipo et al., 2014). The hopanoid-based ordering of lipid bilayer can be improved by structural modification of their polar side chains (Silipo et al., 2014). Hopanoid deficiency may lead to the weakened cell membrane and may affect the other structures spanning cell envelope resulting in impaired lipid ordering which is linked to permeability, fluidity, ion conductivity, cell potential, cell signaling, lateral segregation and disturb the binding of other biomolecules in a membrane (Saenz et al., 2015). Till date, hopanoids are reported to play a role in cell membrane stability, membrane permeability, progression in cell cycle, resistance to antibiotics and help in stress tolerance, but the precise understanding is lacking (Doughty et al., 2011; Kulkarni et al., 2013; Schmerk et al., 2011; Welander et al., 2009). It is unclear how hopanoids contribute to these functions and an effort must be made to elucidate the physiological role of hopanoids in shaping membrane properties and contribution in the membrane-associated functions.

Membrane lipids change the environment of membrane protein which results in alterations of membrane protein activities and there is an effect of the lipid composition on bacterial transport systems. Hopanoids play a crucial role in maintaining lipid order in a cell which can alter the membrane environment (Saenz et al., 2015). Microarray experiment has demonstrated that there is an alteration in BCAA transport, TonB-dependent transport, nitrate transport and polyamine transport which might be because the hopanoid deficient mutant may fail to establish the proton motive force and imbalanced osmotic balance. Results of NPN uptake assay and ATP dependent assay are in line with previous observations which showed the membrane transport is compromised in a hopanoid-deficient mutant of *Methylobacterium extorquens* (Saenz et al., 2015). Energy-dependent transport is deficient in a *Δshc* mutant of *R. palustris* TIE-1 which gives evidence for the link between membrane order and membrane transport. Impaired multidrug efflux may account for sensitivity to chemical stresses. Weakened cell membrane in *Δshc* mutant may create osmotic imbalance and impaired cellular redox potential. Hopanoids are found in the membranes having large proton gradient and therefore acidophiles are known to have high hopanoid content in their membrane (Saenz et al., 2015). Therefore, hopanoids might be playing an essential role in cellular homeostasis and preventing the loss of proton as charged water by increasing the packing of the hydrophobic centers in the cell membrane. Similarly, the upregulation of genes involved in oxidative stress indicates that the hopanoid deficient mutant is under oxidative stress.

In response to external stimuli, bacteria show chemotaxis and flagellar motility which helps the bacteria to reach the favourable environment. Cell membrane plays a crucial role in sensing and passing the message inside the cell. Therefore, in a compromised cell membrane there might be an alteration in signal transduction and motility. *R. palustris* TIE-1 depends on polar flagella for swimming motility which is regulated by a single cell perceiving signal. The flagellar machinery spans the inner and outer membrane in Gram-stain negative bacteria and defect in motility indicate that in *Δshc* mutant the membrane structure is defective, resulting in alteration of membrane-associated function of motility. Twenty-five genes involved in chemotaxis, signal transduction and response to stimuli were downregulated which might be either due to alteration in permeability of cell membrane which affects the sensing ability or direct interaction between hopanoids and certain proteins spanning cell membrane.

Lipid raft in eukaryotes organize signal transduction proteins and enrich in specific lipids such as cholesterol. Cholesterol is one of the critical components in lipid raft and it is known to be involved in various signal transduction processes (Lingwood et al., 2009). Like eukaryotes, prokaryotes contain lipid rafts which orchestrate proteins involved in protein secretion, transportation and signal transduction (Bramkamp and Lopez, 2015). Lipid rafts (microdomains) in bacteria might be involved in signal transduction and membrane organization which explicit the need of exploring the composition and function of bacterial membrane architecture (López and Kolter, 2010). There is a high possibility that bacterial lipid rafts may comprise of hopanoids, as hopanoids are structural and functional analogues to cholesterol. Cell membrane provides a platform to form protein complexes, transport system and sensing receptors which control various cellular processes in the cell. In eukaryotes, it was established that cholesterol regulates the physical properties of a cell membrane and physically interact with various proteins which have a membrane-spanning domain and regulate the functions of various receptor proteins by controlling the membrane curvature and fluidity of membrane (Fantini et al., 2016). The bioinformatics study have thrown light on how cholesterol interacts explicitly with membrane proteins as well as cytosolic proteins, a few of which were further validated by experimental evidence as well (Fantini et al., 2016; Listowski et al., 2015; Sheng et al., 2012).

The computational study has anticipated that diguanylate cyclase has the capability to interact with hopanoids. Diguanylate cyclase catalyses the synthesis of intracellular secondary messenger c-di-GMP (cyclic diguanylate monophosphate) which controls various cellular

processes in a bacterial cell. Cyclic-di-GMP network involves many diguanylate cyclases and many target proteins. C-di-GMP is near universal in bacteria and involved in regulation of a number of complex physiological processes such as motility, progression through cell cycle, cell-cell signalling, secretion, transcription, biofilm formation, bioluminescence, cellulose biosynthesis, virulence and ligand for a riboswitch (Dahlstrom et al., 2015; Paul et al., 2004; Phippen et al., 2014). In *Pseudomonas aeruginosa* PAO1 protein PA4601, a diguanylate cyclase is linked to control a timing of flagella, chemotaxis pathway and dimerization of protein which is required for cyclase activity (Phippen et al., 2014). It is reported that cholesterol interacts with proteins and controls various protein network as well as receptor confirmation and dimerization in membrane protein like G-protein coupled receptor, neurotransmitter receptor for acetylcholine (Fantini et al., 2016). As diguanylate cyclase is reported to be involved in controlling various functions in a bacterial cell and the possible interaction between diguanylate cyclase and hopanoids, there is possible involvement of hopanoids in a signal process in the bacterial cell as cholesterol does in the eukaryotic cell. Therefore, it will be interesting to find out more about the interaction between hopanoids and diguanylate cyclase and other proteins, the role of hopanoids in receptor confirmation and dimerization and possible role in signal transduction. *In-silico* docking is predictive which describes the models of hopanoid-CRAC motif interactions, hence the validation of *in-silico* study needs to be experimentally confirmed. As hopanoids are essential for various membrane related functions, disturbing the membrane order by targeting lipid synthesis can be a possible novel approach in developing new antimicrobials and hopanoid biosynthesis could be a potential target. This work opens many questions and a functional genomics approach has to be used to elucidate answer to these questions and establish the role of hopanoids in various cellular functions.

5. Conclusions

Membrane lipids change the environment of membrane protein which results in alteration of membrane protein activities and various functions. Hopanoid deficiency may lead to the weakened cell membrane and may affect the structures spanning cell envelope resulting in impaired lipid ordering which is linked to permeability, fluidity, ion conductivity, cell potential, cell signaling and lateral segregation, though the mode of action is not known. Understanding the role of hopanoids in determining the structure and functions of the membrane would be pivotal in bridging this gap. The transcriptome data has shown that hopanoid deficiency has led to altered membrane transport. From the experiments, it is explicit that the energy-dependent multidrug transport is flawed in the *Δshc* mutant of *R. palustris* TIE-1 which might be a link between the hopanoids to antibiotic susceptibility. The impaired energy-dependent efflux in hopanoid deficient strain could be a result of either disruption of membrane order or hopanoids might be interacting with proteins and altering their functions. Transcriptome data suggest that hopanoid plays a vital role in maintaining cellular homeostasis. Affected swimming motility in *Δshc* mutant indicates that hopanoids might be playing a direct or indirect role in motility.

Though reports have shown that hopanoid might play a crucial role in lipids ordering, the mechanisms and significance of hopanoid in lipid ordering and signal transduction is poorly understood. The docking study showed that diguanylate cyclase (Rpal_1916 and Rpal_2444) interact with hopanoids (diploptene, diplopterol and tetrahymanol) and might be playing a role in motility and cell signaling in *R. palustris* TIE-1. *In silico* docking is predictive which describes the models of hopanoid-CRAC motif interactions, hence the validation of this docking experiment needs to be confirmed by functional genomics approach. Disturbing the membrane order by targeting lipid synthesis can be a possible novel approach in developing new antimicrobials and hopanoid biosynthesis could be a potential target. Still, the outcome of the interaction between proteins and hopanoids and their role in various membrane related biological functions remains an open question.

Funding information

C.V.R. received funding from the Department of Biotechnology, and Council for Scientific and Industrial Research (CSIR), Government of India.

Conflicts of interests

The authors declare no competing financial interests.

Acknowledgements

T.L. thanks Prof. D. K. Newman, California Institute of Technology and Dr. Paula V. Welander, Environmental Earth System Science, Stanford University for providing *Δshc* mutant and wild type of *R. palustris* TIE-1, respectively. T.L. is thankful to Prof. Aleksander F. Sikorski for sharing three-dimensional structure of MPP1 protein. Tushar acknowledges UGC for SRF fellowship. C.V.R. thanks DBT, and CSIR, Government of India for the award of TATA-Innovative fellowship and research grant, respectively. Infrastructural facilities created under DST FIST and UGC-SAP are acknowledged.

Appendix A. Supplementary data

Supplementary material related to this article can be found, in the online version, at doi:https://doi.org/10.1016/j.micres.2018.10.009.

References

Barak, I., Muchova, K., 2013. The role of lipid domains in bacterial cell processes. Int. J. Mol. Sci. 14, 4050–4065.
Blumenberg, M., Hoppert, M., Krüger, M., Dreier, A., Thiel, V., 2012. Novel findings on hopanoid occurrences among sulfate reducing bacteria: is there a direct link to nitrogen fixation? Org. Geochem. 49, 1–5.
Blumenberg, M., Mollenhauer, G., Zabel, M., Reimer, A., Thiel, V., 2010. Decoupling of bio- and geohopanoids in sediments of the Benguela Upwelling System (BUS). Org. Geochem. 41, 1119–1129.
Blumenberg, M., Oppermann, B.I., Guyoneaud, R., Michaelis, W., 2009. Hopanoid production by *Desulfovibrio bastinii* isolated from oilfield formation water. FEMS Microbiol. Lett. 293, 73–78.
Bramkamp, M., Lopez, D., 2015. Exploring the existence of lipid rafts in bacteria. Microbiol Mol Biol Revh 79, 81–100.
Cvejic, J.H., Bodrossy, L., Kovacs, K.L., Rohmer, M., 2000. Bacterial triterpenoids of the hopane series from the methanotrophic bacteria *Methylocaldum* spp.: phylogenetic implications and first evidence for an unsaturated aminobacteriohopanepolyol. FEMS Microbiol. Lett. 182, 361–365.
Dahlstrom, K.M., Giglio, K.M., Collins, A.J., Sondermann, H., O'Toole, G.A., 2015. Contribution of physical interactions to signaling specificity between a diguanylate cyclase and its effector. mBio 6, e01978–15.
De Maeyer, D., Renkens, J., Cloots, L., De Raedt, L., Marchal, K., 2013. PheNetic: network-based interpretation of unstructured gene lists in E. Coli. Mol. Biosyst. 9, 1594–1603.
Dennis, G., Sherman, B.T., Hosack, D.A., Yang, J., Gao, W., Lane, H., Lempicki, R.A., 2003. DAVID: database for annotation, visualization, and integrated discovery. Genome Biol. 4, R60.
Doughty, D.M., Coleman, M.L., Hunter, R.C., Sessions, A.L., Summons, R.E., Newman, D.K., 2011. The RND-family transporter, HpnN, is required for hopanoid localization to the outer membrane of *Rhodopseudomonas palustris* TIE-1. Proc Natl Acad Sci U S A 108, E1045–51.
Doughty, D.M., Hunter, R.C., Summons, R.E., Newman, D.K., 2009. -Methylhopanoids are maximally produced in akinetes of *Nostoc punctiforme*: geobiological implications. Geobiology 7 (2), 524–532.
Driessen, A.J., de Jong, S., Konings, W.N., 1987. Transport of branched-chain amino acids in membrane vesicles of Streptococcus cremoris. J. Bacteriol. 169, 5193–5200.
Fantini, J., Barrantes, F.J., 2013. How cholesterol interacts with membrane proteins: an exploration of cholesterol-binding sites including CRAC, CARC, and tilted domains. Front. Physiol. 4, 31.
Fantini, J., Di Scala, C., Evans, L.S., Williamson, P.T., Barrantes, F.J., 2016. A mirror code for protein-cholesterol interactions in the two leaflets of biological membranes. Sci. Rep. 6, 21907.
Hannich, J.T., Umebayashi, K., Riezman, H., 2011. Distribution and functions of sterols and sphingolipids. Cold Spring Harb. Perspect. Biol. 3.
Heo, L., Park, H., Seok, C., 2013. GalaxyRefine: protein structure refinement driven by side-chain repacking. Nucleic Acids Res. 41.
Jakob, U., Muse, W., Eser, M., Bardwell, J.C., 1999. Chaperone activity with a redox

switch. Cell 96, 341–352.
Kannenberg, E.L., Perzl, M., Hartner, T., 1995. The occurrence of hopanoid lipids in *Bradyrhizobium* bacteria. FEMS Microbiol. Lett. 127, 255–262.
Kulkarni, g., Wu, Hg., Newman, D.K., 2013. The general stress response factor EcfG regulates expression of the C-2 2 hopanoid methylase HpnP in *Rhodopseudomonas palustris* TIE-1. J. Bacteriol. 195, 2490–2498.
Kulkarni, G., Busset, N., Molinaro, A., Gargani, D., Chaintreuil, C., Silipo, A., Giraud, E., Newman, D.K., 2015. Specific hopanoid classes differentially affect free-living and symbiotic states of Bradyrhizobium diazoefficiens. MBio 6 e01251-15.
Lingwood, D., Kaiser, H.J., Levental, I., Simons, K., 2009. Lipid rafts as functional heterogeneity in cell membranes. Biochem. Soc. Trans. 37, 955–960.
Listowski, M.A., Leluk, J., Kraszewski, S., Sikorski, A.F., 2015. Cholesterol interaction with the MAGUK protein family member, MPP1, via CRAC and CRAC-Like motifs: an in Silico Docking Analysis. PLoS One 10 e0133141.
Loh, B., Grant, C., Hancock, R.E., 1984. Use of the fluorescent probe 1-N-phenylnaphthylamine to study the interactions of aminoglycoside antibiotics with the outer membrane of Pseudomonas aeruginosa. Antimicrob. Agents Chemother. 26, 546–551.
López, D., Kolter, R., 2010. Functional microdomains in bacterial membranes. Genes Dev. 24, 1893–1902.
Noinaj, N., Guillier, M., Barnard, T.J., Buchanan, S.K., 2010. TonB-dependent transporters: regulation, structure, and function. Annu. Rev. Microbiol. 64, 43–60.
Paul, R., Weiser, S., Amiot, N.C., Chan, C., Schirmer, T., Giese, B., Jenal, U., 2004. Cell cycle-dependent dynamic localization of a bacterial response regulator with a novel di-guanylate cyclase output domain. Genes Dev. 18, 715–727.
Phippen, C.W., Mikolajek, H., Schlaefli, H.G., Keevil, C.W., Webb, J.S., Tews, I., 2014. Formation and dimerization of the phosphodiesterase active site of the *Pseudomonas aeruginosa* MorA, a bi-functional c-di-GMP regulator. FEBS Lett. 588, 4631–4636.
Quay, S.C., Oxender, D.L., 1979. The *relA* locus specifies a positive effector in branched-chain amino acid transport regulation. J. Bacteriol. 137, 1059–1062.
Rohmer, M., Bouvier-Navez, P., Ourisson, P.G., 1984. Distribution of hopanoid triterpenes in prokaryotes. J. Microbiol. 130, 1137–1150.
Saenz, J.P., Grosser, D., Bradley, A.S., Lagny, T.J., Lavrynenko, O., Broda, M., Simons, K., 2015. Hopanoids as functional analogues of cholesterol in bacterial membranes. PNAS 112, 11971–11976.
Saenz, J.P., Sezgin, E., Schwille, P., Simons, K., 2012a. Functional convergence of hopanoids and sterols in membrane ordering. PNAS 109, 14236–14240.
Saenz, J.P., Wakeham, S.G., Eglinton, T.I., Summons, R.E., 2011. New constraints on the provenance of hopanoids in the marine geologic record: bacteriohopanepolyols in marine suboxic and anoxic environments. Org. Geochem. 42, 1351–1362.
Saenz, J.P., Waterbury, J.B., Eglinton, T.I., Summons, R.E., 2012b. Hopanoids in marine cyanobacteria: probing their phylogenetic distribution and biological role. Geobiology 10, 311–319.
Schmerk, C.L., Bernards, M.A., Valvano, M.A., 2011. Hopanoid production is required for low-pH tolerance, antimicrobial resistance, and motility in Burkholderia cenocepacia. J. Bacteriol. 193, 6712–6723.
Shah, P., Swiatlo, E., 2008. A multifaceted role for polyamines in bacterial pathogens. Mol. Microbiol. 68, 4–16.
Sheng, R., Chen, Y., Yung Gee, H., Stec, E., Melowic, H.R., Blatner, N.R., Tun, M.P., Kim, Y., Kallberg, M., Fujiwara, T.K., Hye Hong, J., Pyo Kim, K., Lu, H., Kusumi, A., Goo Lee, M., Cho, W., 2012. Cholesterol modulates cell signaling and protein networking by specifically interacting with PDZ domain-containing scaffold proteins. Nat. Commun. 3, 1249.
Silipo, A., Vitiello, G., Gully, D., Sturiale, L., Chaintreuil, C., Fardoux, J., Gargani, D., Lee, H.I., Kulkarni, G., Busset, N., Marchetti, R., Palmigiano, A., Moll, H., Engel, R., Lanzetta, R., Paduano, L., Parrilli, M., Chang, W.S., Holst, O., Newman, D.K., Garozzo, D., D'Errico, G., Giraud, E., Molinaro, A., 2014. Covalently linked hopanoid-lipid A improves outer-membrane resistance of a *Bradyrhizobium* symbiont of legumes. Nat. Commun. 5, 5106.
Talbot, H.M., Summons, R., Jahnke, L., Cockell, C.S., Rohmer, M., Farrimond, P., 2008. Cyanobacterial bacteriohopanepolyol signatures from cultures and natural environmental settings. Org. Geochem. 39, 232–263.
Tam, R., Saier Jr, M.H., 1993. Structural, functional, and evolutionary relationships among extracellular solute-binding receptors of bacteria. Microbiol. Rev. 57, 320–346.
Tank, M., Bryant, D.A., 2015. *Chloracidobacterium thermophilum* gen. nov., sp. nov.: an anoxygenic microaerophilic chlorophotoheterotrophic acidobacterium. Int. J. Syst. Evol. Microbiol. 65, 1426–1430.
Wei, J.H., Yin, X., Welander, P.V., 2016. Sterol synthesis in diverse bacteria. Front. Microbiol. 7, 990.
Welander, P.V., Hunter, R.C., Zhang, L., Sessions, A.L., Summons, R.E., Newman, D.K., 2009. Hopanoids play a role in membrane integrity and pH homeostasis in *Rhodopseudomonas palustris* TIE-1. J. Bacteriol. 191, 6145–6156.
Zhang, Y., 2008. I-TASSER server for protein 3D structure prediction. BMC Bioinformatics 9, 40.